

# DISTRIBUTED SEEDING FOR NARROW-LINEWIDTH HARD X-RAY FREE-ELECTRON LASERS\*

D.C. Nguyen<sup>#</sup>, P.M. Anisimov, C.E. Buechler, J.W. Lewellen, Q.R. Marksteiner  
LANL, Mail Stop H851, Los Alamos, New Mexico, USA

## Abstract

We describe a new FEL line-narrowing technique called distributed seeding (DS), using Si(111) Bragg crystal monochromators to enhance the spectral brightness of the MaRIE hard X-ray free-electron laser. DS differs from self-seeding in three important aspects. First, DS relies on spectral filtering of the radiation at multiple locations along the undulator, with a monochromator located every few power gain lengths. Second, DS performs filtering early in the exponential gain region before SASE spikes start to appear in the radiation longitudinal profile. Third, DS provides the option to select a wavelength longer than the peak of the SASE gain curve, which leads to improved spectral contrast of the seeded FEL over the SASE background. Time-dependent Genesis simulations show the power-vs-z growth curves for DS exhibit behaviors of a seeded FEL amplifier, such as exponential growth region immediately after the filters of the seeding approaches considered, the two-stage DS spectra produce the highest contrast of seeded FEL over the SASE background and that the three-stage DS provides the narrowest linewidth with a relative spectral FWHM of  $8 \times 10^{-5}$ .

## INTRODUCTION

X-ray free-electron lasers (XFELs) routinely operate in the SASE mode, whereby the radiation power grows exponentially with distance in a long undulator as a single electron bunch amplifies its own undulator radiation all the way to saturation. The radiation slips ahead of the electrons by the slippage distance  $N_u \lambda_0$ , where  $N_u$  is the number of undulator periods and  $\lambda_0$  is the resonance wavelength, forming randomly distributed wave-packets within a single radiation pulse. In the exponential gain regime, these wave-packets develop into high-intensity longitudinal spikes, each of which is coherent within a coherence length given by

$$l_c = \frac{\lambda_0}{6\sqrt{\pi\rho}} \sqrt{\frac{z}{L_G}},$$

where  $\lambda_0$  is the resonance wavelength,  $z$  is the distance traversed by the electrons in the undulator,  $L_G$  is the 1D power gain length, and  $\rho$  is the Pierce parameter. At saturation ( $z \sim 20 L_G$ ), the coherence length is

$$l_c^{sat} \approx \frac{\lambda_0}{2\sqrt{\pi\rho}}.$$

For an XFEL with sub-Angstrom output wavelength,  $\rho$  is on the order of  $5 \times 10^{-4}$ , and thus the coherence length at saturation is on the order of 20 nm. The mean separation between these spikes is  $\Delta z_{spike} \leq 2\pi l_c$ , or about 100 nm, much shorter than the overall radiation pulse length (~tens of  $\mu\text{m}$ ). The frequency spectrum of a SASE XFEL consists of hundreds of narrow spectral lines, each being the Fourier transform of the radiation overall temporal duration, within an envelope that is the Fourier transform of the individual temporal spikes. The overall SASE spectrum has a relative bandwidth FWHM of

$$\frac{\Delta\lambda}{\lambda_0} = \frac{4\ln 2}{\sqrt{\pi}} \rho,$$

or about 0.1% for the typical  $\rho$  of an XFEL. The large bandwidth and poor temporal coherence of the SASE XFEL preclude its use in applications that require a high degree of longitudinal coherence such as three-dimensional coherent X-ray diffractive imaging.

SASE self-seeding has been studied and successfully employed to reduce the XFEL bandwidth to a fraction of an electron volt [1-5]. This technique relies on monochromatizing the SASE radiation from the first part of the undulator and then re-injecting the monochromatic seed into the second part of the undulator for amplification. Hard X-ray self-seeding can be performed either with a Bragg crystal monochromator as suggested by Saldin *et al.* [1], or a diamond wake crystal as suggested by Geloni *et al.* [2]. Self-seeding at both hard and soft X-ray energies has been demonstrated at the Linac Coherent Light Source [3, 4], where the seeded FEL spectra typically exhibit a narrow spectral line on top of a broadband SASE background. Geloni *et al.* also proposed using cascade self-seeding [5] to improve the contrast of self-seeded FEL over SASE.

We present a new concept of distributed seeding (DS) using multiple silicon Bragg crystal monochromators. DS differs from SASE self-seeding in three important aspects. First, DS relies on spectral filtering of the radiation at more than one location along the undulator. For this study, we consider both the two-filter and three-filter DS with a spectral filter located every five power gain lengths. Second, DS performs filtering early in the exponential gain region before SASE spikes start to appear in the radiation longitudinal profile to ensure the

\*Work supported by the US DOE / NNSA under contract DE-AC52-06NA25396.  
#dcnguyen@lanl.gov



Figure 1: Schematic of the MaRIE XFEL undulator with 14 FODO periods and three locations for the spectral filters.

radiation is dominated by a coherent seed and not SASE noise. Third, DS provides the option to select a wavelength longer than the peak of the SASE gain curve, which leads to improved spectral contrast of the seeded FEL over the SASE background.

### MaRIE X-RAY FEL

The MaRIE XFEL is a proposed hard X-ray FEL driven by 12-GeV electron beams to generate coherent 42-keV photons. At a resonance wavelength of  $0.2936 \text{ \AA}$ , four Si(111) Bragg crystals, each deflecting the X-ray beam by  $5.4^\circ$ , can be used in a four-bounce crystal monochromator (4BCM). The 4BCM increases the X-ray beam path by 1.2 ps (0.36 mm), which can be matched by delaying the electron beams in a small-angle bypass chicane that will be described later in this paper. The bypass chicane  $R_{56}$  is sufficiently large to erase the FEL-induced microbunching so that each electron bunch behaves like a fresh bunch upon entering the next undulator segment.

Using time-dependent numerical FEL simulations with Genesis 1.3 [6], we model the DS FEL with either two or three monochromators along the undulator. Two cases of the two-filter configuration are studied, one with the first filter at the end of the first two FODO periods, and the other at the end of the four FODO periods. The three-filter configuration involves filtering at every two FODO periods starting at the end of the first two FODOs. We present the number of photons versus distance along the undulator for these three cases.

The electron beams traversing the bypass chicane are expected to experience loss of beam brightness caused by coherent synchrotron radiation (CSR) and to a lesser extent, by incoherent synchrotron radiation (ISR). Beam dynamic simulations using Elegant [7] to compute the effects of CSR and ISR on the beam energy, energy spread and emittance in each bypass chicane. These simulations show the dominant effect is CSR-induced reduction in the peak current and slice energy in the latter part of the electron bunch. CSR also causes a small increase in the slice emittance but this has no noticeable effects on the FEL performance.

Figure 1 shows the MaRIE XFEL undulator with fourteen FODO periods and three locations for the spectral filters. The two-filter configurations under study are AB, with the monochromators at locations A and B, and BC with the filters at locations B and C. The three-stage configuration ABC has monochromators at all three locations.

Figure 2a illustrates the small-angle, four-dipole chicane to temporally delay the electron beam to synchronize it with the X-ray beam, including the monochromator (in between the middle dipoles). The dipole length is 35 cm and the center-to-center distance between

the first and second (also the third and fourth) dipoles is 3.3 m. The four-bounce crystal monochromator is illustrated in Fig. 2b. The first and last Si(111) crystals are flat; however, the second and third crystals are curved to produce a  $0.7 \mu\text{m}$  rms radius at the slit in the middle of the 4BCM. The function of the slit is to select a narrow spectrum at the long wavelength and reject the SASE signal.

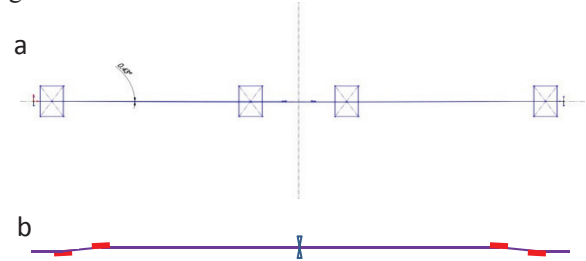


Figure 2: a) The four-dipole bypass chicane with the 4BCM in between the two middle dipoles; b) expanded view of the 4BCM showing the four Si(111) crystals in red and the slit in blue. The total length of the bypass chicane (2a) is 8.63 m whereas the length of the 4BCM (2b) is 0.4 m.

By filtering the undulator radiation early in the exponential growth curve, we can increase the throughput of the 4BCM at the longer wave as the undulator radiation at this point is dominated by longer wavelength radiation. Figure 3 plots the averaged single-shot undulator radiation spectrum at the end of four gain lengths (blue), the averaged SASE power (red), and the spectral response of the four-crystal monochromator with its wavelength centered at  $0.2940 \text{ \AA}$  (green). Since the DS signal is at a longer wavelength but SASE is shifted toward shorter wavelength, the contrast of DS over SASE is enhanced.

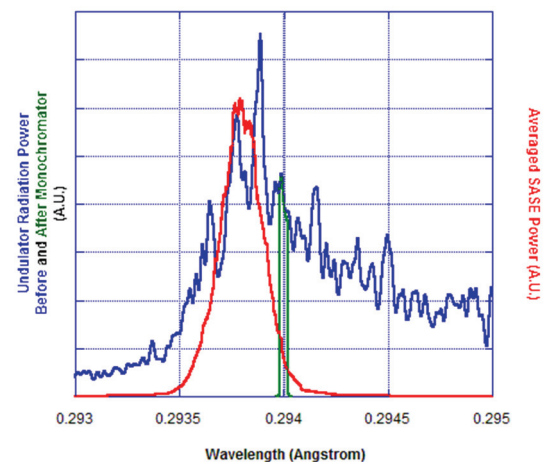


Figure 3: The undulator radiation spectrum before (blue) and after (green) the 4BCM, and the average SASE signal in the exponential gain regime (red).

We anticipate that bending the electron beams in the bypass chicane will result in beam quality degradations, mainly caused by coherent synchrotron radiation (CSR) and to a lesser extent, by incoherent synchrotron radiation (ISR). Beam dynamic simulations using Elegant [7] to compute the effects of CSR and ISR on the beam energy, energy spread and emittance in each bypass chicane, show the dominant effect is CSR-induced reduction in the peak current and slice energy (gamma) in the latter part of the electron bunch (Fig. 4), which can be compensated for by a small taper in the undulator  $K$  parameter. CSR also causes a negligible increase in the slice emittance with no noticeable effects on the FEL performance.

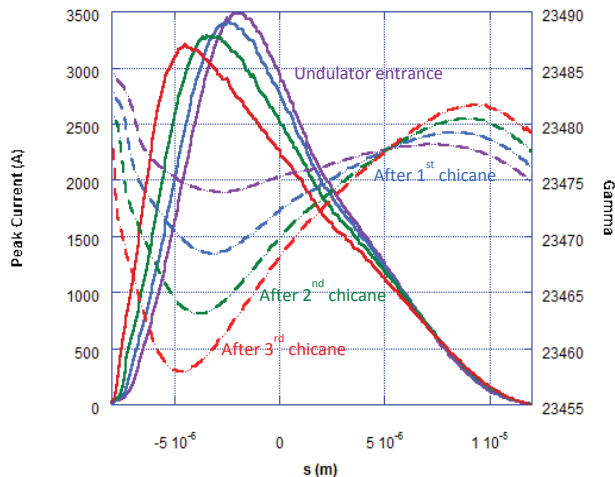


Figure 4: The CSR-induced reduction in peak current (solid lines) and slice beam gamma (dashed lines) as functions of the electron bunch position at three different undulator locations: purple = undulator entrance, blue = after the first chicane, green = after the second chicane, and red = after the third chicane.

### SIMULATIONS

We use the full 4D (time-dependent) Genesis to predict the DS performance using the MaRIE XFEL parameters [8]. Numerically, the on-axis power and phase of the Genesis output at the ends of the second, fourth and sixth FODO cells was used with the assumption that the radiation beam has full coherence across the transverse profile. Fourier transform was applied to the complex electric field to produce the radiation spectrum, which is then multiplied by the spectral response of the four silicon crystals to produce the filtered spectrum. The latter is Fourier-transformed back into the time domain and then serves as the monochromatic seed for the subsequent undulator segments. Figure 5 plots the log of the numbers of photons versus undulator length for the two-filter DS cases (AB and BC) and the three-filter DS case ABC.

### CONCLUSIONS

We have shown via time-dependent 3D Genesis simulations that the DS technique, using multiple Bragg crystal monochromators, can provide a high degree of temporal coherence for the MaRIE XFEL. The DS confi-

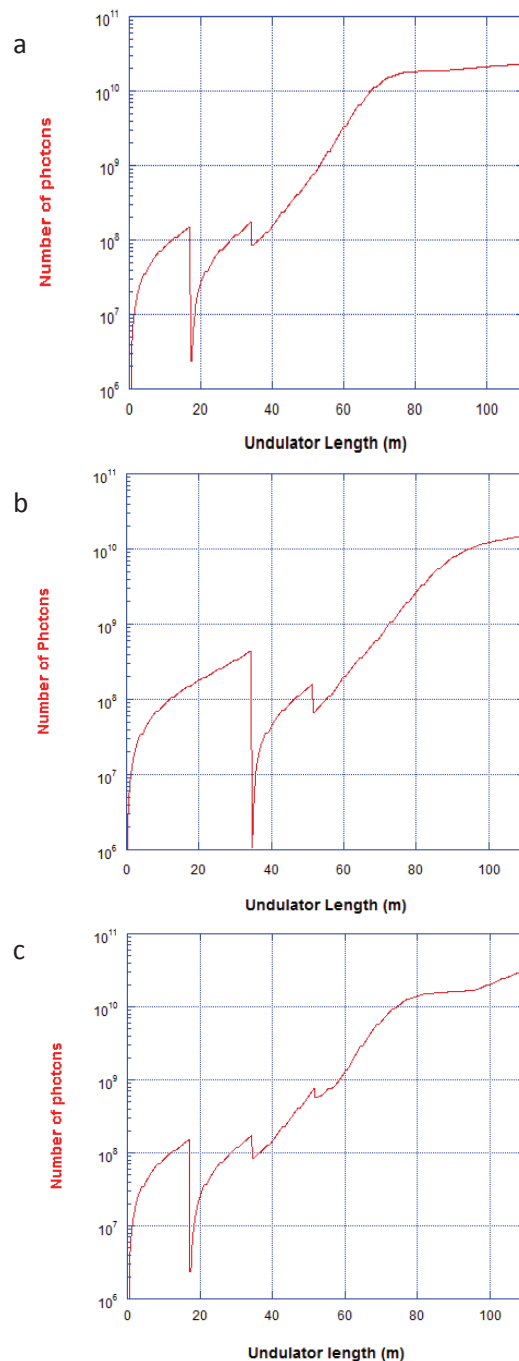


Figure 5: a) Plots of the number of photons versus undulator length for the DS configurations a) two-filter AB; b) two-filter BC; and c) three-filter ABC.

guration with only two monochromators already achieves a 10X enhancement in X-ray brightness compared with the traditional SASE technique and produces a narrow-line seeded FEL spectrum with good contrast between the monochromatic output and the SASE background. The DS configuration with three monochromators provides additional spectral narrowing but with a slight increase in the SASE background. Both the two-stage and three-stage DS FEL output has a filled-in longitudinal profile with a coherence length on the order of 200 nm. It also exhibits a

power-versus-z plot characteristic of a true seeded amplifier FEL. For the MaRIE XFEL, the two-stage DS technique appears to be the more practical than the three-stage DS as a spectral line narrowing technique.

We have performed Elegant simulations to model beam degradation due to CSR and ISR in the chicanes that are used to delay the electron bunch to match with the X-ray delays in the monochromators. Although the CSR-induced beam degradations are small, they are cumulative with the number of chicanes. The dominant effect is a steady reduction in the peak current and the slice electron beam energy in the region of the electron bunch where most of the FEL interaction occurs, i.e., at the electron beam energy minimum near the end of the bunch. This cumulative change in beam energy requires that the undulator  $K_{\text{rms}}$  parameter be reduced (step-tapered) to maintain the FEL resonance.

One of the key features of the DS method is the ability to tune the central wavelength away from the SASE resonance wavelength. A combination of the judicious choice of the central wavelength and the undulator  $K_{\text{rms}}$  parameters can put the DS central wavelength in between the SASE backgrounds of different undulator stages, thereby enabling subsequent spectral filtering to improve the contrast between the seeded spectral line and the SASE background.

## ACKNOWLEDGMENTS

The authors benefited from helpful discussions with Bruce Carlsten, Richard Sheffield and Nikolai Yampolsky at LANL, and Craig Ogata and Yuri Shvyd'ko at Argonne National Laboratory. This research was funded by the Los Alamos National Laboratory Matter-Radiation Interactions in Extremes (MaRIE) program, led by Cris Barnes and John Tapia.

## REFERENCES

- [1] E.L. Saldin, E.A. Schneidmiller, Yu.V. Shvyd'ko, and M.V. Yurkov, *Nucl. Instr. Meth. Phys. Res. A* **475** 357-362 (2001).
- [2] G. Geloni, V. Kocharyan, and E. Saldin, *J. Mod. Opt.*, **58**:1391–1403 (2011).
- [3] J. Amann *et al.*, *Nature Photonics* **6**, 693-698 (2012).
- [4] D. Cocco *et al.*, in *Proc. SPIE 8849, "X-ray lasers and coherent X-ray sources,"* 88490A-1, (2013).
- [5] G. Geloni *et al.*, *DESY* **10-080** (2010).
- [6] S. Reiche, *Nucl. Instr. Meth. Phys. Res. A* **429** 243-248 (1999).
- [7] M. Borland, *Phys. Rev. ST Accel. Beams* **4**, 070701 (2001).
- [8] J.W. Lewellen *et al.*, these proceedings, paper MOP062.